Biosensors and Bioelectronics 75 (2016) 188–195

Contents lists available at ScienceDirect

Biosensors and Bioelectronics

journal homepage: www.elsevier.com/locate/bios

Aptamer–MIP hybrid receptor for highly sensitive electrochemical detection of prostate specific antigen

Pawan Jolly [a,1], Vibha Tamboli [b,1], Robert L. Harniman [c], Pedro Estrela [a], Chris J. Allender [b], Jenna L. Bowen [b,*]

[a] Department of Electronic & Electrical Engineering, University of Bath, Bath BA2 7AY, United Kingdom
[b] School of Pharmacy and Pharmaceutical Sciences, Cardiff University, Cardiff CF10 3NB, United Kingdom
[c] School of Chemistry, University of Bristol, Cantock's Close, Bristol BS8 1TS, United Kingdom

ARTICLE INFO

Article history:
Received 1 July 2015
Received in revised form
13 August 2015
Accepted 20 August 2015
Available online 21 August 2015

Keywords:
Molecular imprinting
Aptamer
Electrochemical impedance spectroscopy
Prostate cancer
Prostate specific antigen

ABSTRACT

This study reports the design and evaluation of a new synthetic receptor sensor based on the amalgamation of biomolecular recognition elements and molecular imprinting to overcome some of the challenges faced by conventional protein imprinting. A thiolated DNA aptamer with established affinity for prostate specific antigen (PSA) was complexed with PSA prior to being immobilised on the surface of a gold electrode. Controlled electropolymerisation of dopamine around the complex served to both entrap the complex, holding the aptamer in, or near to, it's binding conformation, and to localise the PSA binding sites at the sensor surface. Following removal of PSA, it was proposed that the molecularly imprinted polymer (MIP) cavity would act synergistically with the embedded aptamer to form a hybrid receptor (apta–MIP), displaying recognition properties superior to that of aptamer alone. Electrochemical impedance spectroscopy (EIS) was used to evaluate subsequent rebinding of PSA to the apta–MIP surface. The apta–MIP sensor showed high sensitivity with a linear response from 100 pg/ml to 100 ng/ml of PSA and a limit of detection of 1 pg/ml, which was three-fold higher than aptamer alone sensor for PSA. Furthermore, the sensor demonstrated low cross-reactivity with a homologous protein (human Kallikrein 2) and low response to human serum albumin (HSA), suggesting possible resilience to the non-specific binding of serum proteins.

1. Introduction

Whilst antibodies remain the molecular recognition workhorse of choice for many laboratory assays and bio-sensing devices, their use can impose limitations on both technology adoption and resulting applications. Issues such as cost, availability, stability, robustness and engineerability all must be taken into consideration in assay or device design. One long-championed 'alternative' to antibodies has been molecular imprinting, yet despite its many supporters the approach has had little impact as a viable bioanalytical tool to date. At the heart of this rather disappointing picture is a critical limitation, that conventional non-covalent molecular imprinting is fundamentally unsuitable as a mean for preparing antibody-alternatives for use in water; the most important solvent with regards to commercially relevant applications of molecular recognition. For proteins in particular, where molecular size brings issue of permanent entrapment and kinetic limitations (Turner et al., 2006), molecular imprinting, despite a huge amount of attention by researchers, has been unable to find any foothold in what is a huge commercial market.

One approach that has shown promise in the area of macromolecular imprinting is the integration of biomolecules, with inherent affinity for a particular protein target, into a MIP polymer scaffold, giving rise to a so-called hybrid-MIP system. The hypothesis underpinning the creation of such hybrid systems is that the 'templating' effects will give rise to affinities and/or selectivity above and beyond that demonstrated by the biomolecule alone. The hybrid-MIP strategy was first proposed for the detection of lipopolysaccharide (LPS) using the cyclic peptide polymyxin (Bowen, 2011) and has also been reported for concanavalin A detection using mannose (Dechtrirat et al., 2014).

Another type of bioreceptor that has been employed in hybrid-MIP approaches is the DNA aptamer (Bai and Spivak, 2014; Poma et al., 2015). DNA aptamers are short, stable oligonucleotide sequences possessing high affinity and specificity for particular

* Corresponding author.
E-mail addresses: P.Jolly@bath.ac.uk (P. Jolly), Tamboliv@cardiff.ac.uk (V. Tamboli), rob.harniman@bristol.ac.uk (R.L. Harniman), P.Estrela@bath.ac.uk (P. Estrela), Allendercj@cardiff.ac.uk (C.J. Allender), Bowenjl2@cardiff.ac.uk (J.L. Bowen).
[1] These authors contributed equally to the manuscript.

http://dx.doi.org/10.1016/j.bios.2015.08.043

molecular targets (McCauley et al., 2003). DNA-aptamers have, in their own right, been extensively used as alternatives to antibodies in biosensing applications ('Aptasensors') (Rodriguez et al., 2005; Maehashi et al., 2007; Jolly et al., 2015a). Despite their inherent stability DNA aptamers are still subject to nuclease degradation (Keum and Bermudez, 2009) and an additional benefit of their incorporation within hybrid polymer systems has been shown to be an increase in stability (Poma et al., 2015).

This study aims to develop a hybrid-MIP receptor for use in an electrochemical sensor targeting the quantitative analysis of prostate specific antigen (PSA). PSA is a 30–33 KDa serine protease secreted by the prostate gland, the levels of which are elevated in men with prostate cancer (PCa) (Heidenreich et al., 2014a). Despite well-documented limitations (Hayes and Barry, 2014), PSA remains most commonly used biomarker for PCa screening, monitoring the effectiveness of treatment and assessing likelihood of remission post treatment (Hayes and Barry, 2014; Heidenreich et al., 2014b).

Unlike previous studies, this work does not rely on the chemical modification of the biorecognition motif in order to make it 'polymerisable' (Poma et al., 2015). In the current study, a preformed 'thiolated DNA aptamer–PSA' complex is immobilised onto the surface of a clean gold electrode. By surface immobilising the complex prior to polymerisation, the order and homogeneity of the resulting hybrid system is favoured. Subsequently multiple layers of electropolymerised polydopamine were deposited to act as a supportive and protective scaffold for the aptamer and also to restrict the aptamer in, or near to, its preferred binding conformation. It was also anticipated that the polymer layer would contribute to PSA binding by partially entrapping the protein in a conventional surface-confined imprinted cavity. It was hypothesised that following PSA (template) removal, contributions to rebinding from both the restrained aptamer and the polymer binding pocket would result in a templated hybrid surface (apta–MIP) with PSA rebinding properties superior to aptamer alone. Electrochemical impedance spectroscopy (EIS) was used to evaluate the binding characteristics of the apta–MIP sensor for PSA and also for a closely related protein possessing ~80% sequence homology.

2. Materials and methods

2.1. Instruments and reagents

Electrochemical measurements were performed using a μAUTOLAB III/FRA2 potentiostat (Metrohm Autolab, The Netherlands) with a three-electrode configuration comprising a Ag/AgCl reference electrode (BASi, USA), connected via a salt bridge filled with 10 mM phosphate buffer saline (PBS) pH 7.4 containing 150 mM NaCl and 10 mM KCl, and a platinum (Pt) counter electrode (ALS, Japan). The electrochemical impedance spectrum was measured in 10 mM PBS (pH 7.4) measurement buffer containing 10 mM ferro/ferricyanide $[Fe(CN)_6]^{3-/4-}$ in the frequency range 10 kHz to 100 mHz, with a 10 mV a.c. voltage superimposed on a bias d.c. voltage of 0.2 V vs Ag/AgCl reference electrode (corresponding to the formal potential of the redox couple). All measurements were performed at room temperature.

Thiol terminated PSA binding DNA aptamer (5′-HS–$(CH_2)_6$–TTT TTA ATT AAA GCT CGC CAT CAA ATA GCT TT-3′) was obtained from Sigma-Aldrich, UK. PSA was obtained from Merck Chemicals Ltd., UK. Human glandular Kallikrein 2 (hK2) was obtained from RnD Systems, UK. All other reagents were of analytical grade and obtained from Sigma-Aldrich, UK. All aqueous solutions were prepared using 18.2 MΩ cm ultra-pure water from a Milli-Q system with a Pyrogard filter (Millipore, MA, USA).

2.2. Apta–MIP preparation

Gold electrodes were cleaned and activated as detailed in the Supporting information (Section S2). Thiolated aptamer was activated at 95° C for 10 min before being gradually cooled to room temperature for 30 min (Savory et al., 2010). Thereafter, 1 μM aptamer in TBST buffer (10 mM Tris–HCl, 10 mM KCl, 10 mM $MgCl_2$, 0.05% Tween 20, pH 7.4)) was incubated with 1 μg/ml of PSA for 1 h at 37 °C. Clean gold electrodes were then exposed to the resulting aptamer–PSA complex solution for one hour before being rinsed carefully with ultra pure water. To saturate any free aptamers on the surface and favour the aptamer–PSA complex formation the electrodes were subsequently incubated with 1 μg/ml PSA for an additional 30 min before rinsing with ultrapure water and drying under nitrogen.

The molecular imprinting step was performed by electropolymerising dopamine on to the aptamer–PSA modified electrode using a method adapted from literature (Liu et al., 2006). Briefly, 10 mM PBS buffer (pH 7.4) containing 5 mM dopamine was degassed with nitrogen (10 min) and then electropolymerised using cyclic voltammetry (13 cycles, −0.5 to 0.5 V vs Ag/AgCl, scan rate of 20 mV/s). Electrodes were rinsed with water and washed (with stirring) overnight in washing solution (5% v/v acetic acid and 5% w/v sodium dodecyl sulphate (SDS) in water) to remove the PSA template. Electrodes were then rinsed with water to remove residual acid and detergent before being allowed to stabilise in measurement buffer (10 mM PBS (pH 7.4) containing 10 mM $[Fe(CN)_6]^{3-/4-}$ and 0.05% v/v Tween 20). A non-imprinted 'control' electrode (apta–NIP) was prepared in the same way but in the absence of PSA.

2.3. Sensor performance

To evaluate sensor performance, electrodes were mounted in a three-electrode configuration with the apta–MIP or apta–NIP as the working electrode. Following baseline stabilisation, the electrodes were exposed to 100 μl of a range of PSA concentrations (10^{-1}–10^{6} pg/ml) in measurement buffer. Electrochemical impedance spectroscopy (EIS) was used to measure capacitive changes at the electrode/electrolyte interface resulting from PSA re-binding. Human Kallikrein 2 (hK2) was used to evaluate binding specificity. The sensors were also challenged with varying concentrations of human serum albumin (HSA, prepared in the same buffer) to study non-specific binding effects.

2.4. Microscopy

The thickness and root mean squared (RMS) roughness of washed and unwashed apta–MIP films on gold-coated glass slides (Au thickness 150 nm) were determined by atomic force microscopy (AFM) (Multimode Nanoscope V, Bruker, CA, USA). Prior to analysis, both samples were rinsed with MilliQ water and dried with a lateral flow of nitrogen. Small scratches were made in each film using a sharp cantilever tip, < 10 nm, on a rigid cantilever of spring constant 42 N/m (NuSENSE, NuNano, Bristol, UK). Keeping the applied force below 50 nN ensured that the scratching process did not damage the underlying gold film. The depth of the resulting scratches was investigated at high resolution utilising a compliant cantilever of spring constant 0.4 N/m with a sharper tip, < 2 nm, (SCANASYST-AIR-HR, Bruker, CA, USA). The greater compliance of the cantilever allows interaction forces normal to the sample to be maintained in the region of a few hundred pN, thus minimising possible film compression. Images were collected at a resolution of 2 nm/pixel.

3. Results and discussion

3.1. Fabrication of hybrid DNA aptamer–MIP surfaces

Fig. 1 provides a schematic of the fabrication technique (a–d) and a series of voltammograms illustrating changes in the electrical property of the gold electrode during the modification process (e). Distinct oxidation and reduction peaks of the redox couple at high current levels were observed (Fig. 1e, black line) demonstrating the conducting nature of the bare electrode. Following immobilisation of the aptamer–PSA complex a reduction in current, and a shift in peak voltage, were observed (Fig. 1e, red line). This is attributed to the formation of a resistive aptamer–PSA self-assembled monolayer (SAM) on the gold surface. Since immobilisation of aptamer alone has been shown to produce a densely packed surface with reduced PSA binding efficiency (Formisano et al., 2015), it was hypothesised that the immobilisation of the aptamer–PSA complex would give rise to a less densely packed surface, due to steric hindrance provided by PSA, favouring electropolymerisation at the electrode surface and subsequent PSA rebinding.

When preparing MIP sensor surfaces it is desirable that the polymer layer is thin so as to enable efficient transduction of surface binding events to the underlying electrode (Panasyuk et al., 1999). One strategy that has been successfully used to produce thin and homogenous polymer films is the electropolymerisation of electroactive monomers (Blanco-López et al., 2004). In the current study, dopamine was selected as the monomer due to its low oxidation/reduction potential, meaning that electropolymerisation could be performed in the presence of the immobilised aptamer–PSA complex without fear of oxidising the thiol linkage that immobilises it on the surface (Łuczak, 2008). In addition, it was anticipated that the hydroxyl and amide functional groups of polydopamine would form non-covalent interactions with PSA, thus conferring a second level of recognition acting synergistically with the aptamer. Electropolymerisation of dopamine (see Fig. S1 in Supporting information) also produced a compact and rigid polymer that is a good insulator; a property that is beneficial for capacitive measurements (Ball et al., 2012).

An important parameter in this study was polymer thickness. If significantly greater than the aptamer–PSA complex height then the on/off kinetics may be slow or even completely inhibited if the protein becomes permanently entrapped. If the polymer layer was much thinner than the height of the aptamer–PSA complex then little molecular imprinting contribution would be predicted. The number of electropolymerisation cycles was therefore varied from 7 to 25 cycles in order to identify an optimal polymer thickness. Based on these experiments, AFM measurements and an approximation of aptamer–PSA complex size, optimal polymer thickness was predicted to be ~10 nm. This polymer thickness was obtained with 13 cycles of electropolymerisation. Aptamer–PSA template height calculation is provided in Supporting information (Section S1).

Post polymerisation, a significant reduction in peak current was observed (Fig. 1e, blue curve) indicative of the presence of an insulating poydopamine layer. Following washing of the imprinted electrode, a small increase in peak current was observed (~0.6 μA) (Fig. 1e inset), however the peak current remained significantly lower than for the bio-functionalised gold electrodes prior to polymerisation suggesting polymer remained on the surface post-washing. It is proposed that the small increase in peak current was not only a consequence of PSA removal but also the loss of a small amount of loosely associated polymer. It has

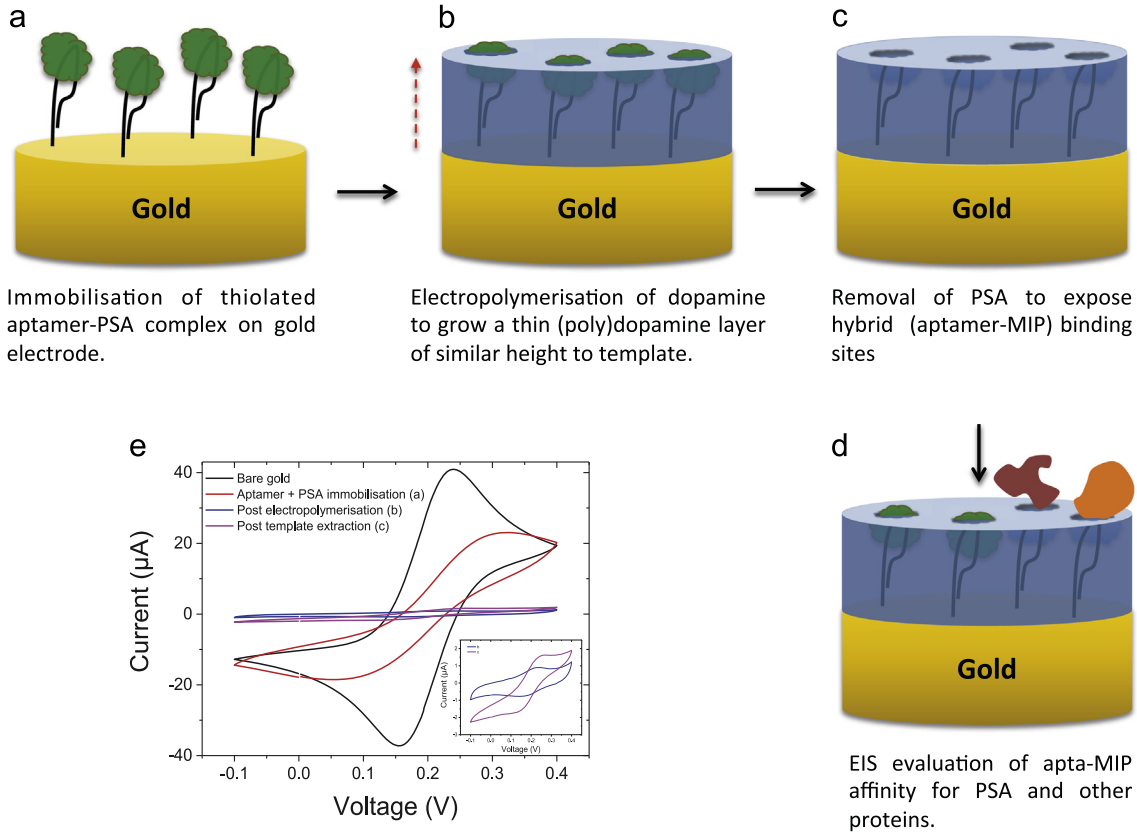

Fig. 1. Schematic representation of the sensor fabrication. The aptamer–PSA complex is first immobilised on the gold surface utilising thiol chemistry (a) with subsequent electropolymerisation of dopamine around the complex to produce a molecularly imprinted surface (b). Washing of the electrode allows for removal of PSA whilst retaining aptamer-lined, imprinted polymeric cavities, the so-called "apta–MIP" (c). Reintroduction of the template molecule results in rebinding within the imprinted sites (d). Cyclic voltammetry monitoring of the fabrication process (e). (For interpretation of the references to colour in this figure, the reader is referred to the web version of this article.)

previously been reported that polydopamine auto-polymerises in solution and it is possible that the polymer that was lost from the electrode during the washing step was the auto-polymerised polydopamine that had become loosely and non-specifically associated with the electrode surface (Lynge et al., 2011). A reduction in charge transfer resistance (R_{ct}) of approximately 50 kΩ and 20 kΩ was observed following washing of the apta–MIP and apta–NIP respectively, again suggesting the loss of both protein and polymer. Chronocoulometry was performed to allow estimation aptamer density pre and post washing (see Supporting information Section S2 and Figs. S2 and S3). No significant changes in aptamer density were observed post washing indicating presence of aptamer on the electrode surface.

3.2. Physical characterisation of apta–MIP sensor

Tapping mode atomic force microscopy (AFM) was performed in order to characterise the polymer layer. Post-polymerisation a clear difference in wettability was observed between the apta–MIP surface (hydrophilic) and bare-gold (hydrophobic), which remained unchanged post-washing of the apta–MIP suggesting the presence of a stable polymer layer. The root mean square (RMS) roughness of the bare-gold surface was 2.0 nm (see Fig. S4 in Supporting information) and this increased to 2.6 nm following the formation of the apta–MIP (Fig. 2). Washing of the apta–MIP with SDS and acetic acid resulted in a reduction in roughness to 2.2 nm. The thickness of the polymer layer, measured as the step-depth between the base of a scratch and the flat surface of the top of the film, was 10.61 nm ($n=10$; SD 1.23 nm) before washing, which decreased to 7.49 nm ($n=10$; SD 0.42 nm) post washing. This provides further evidence that washing to remove the template (PSA) also brought about some loss of loosely associated polymer. It should be noted that measurements were carried out on dehydrated polymer surfaces. It is therefore likely that this is an underestimate of their 'in-use' thickness given that polydopamine has been reported to swell 1.12–1.25 times when hydrated (Ho and Ding, 2013; Liu et al., 2015; Bernsmann et al., 2009).

3.3. Electrochemical performance of apta–MIP sensor

Electrochemical impedance spectroscopy (EIS) was used in this study to measure capacitive changes at the electrode/electrolyte interface as a result of PSA re-binding. Fig. 3a shows the Nyquist plots of the system upon the addition of different PSA concentrations. The data can be best fitted using an equivalent circuit comprising two $R\|C$ (resistance in parallel with capacitance) circuits in series, R_s $(R_1\|C_1)$ $(R_2\|C_2)$, where R_s is the solution resistance. C_2 can be replaced by a constant phase element (CPE) with impedance $Z_{CPE}\equiv 1/Q_{CPE}(j\omega)^n$, which accounts for a for suitable fitting of the data. The two semicircles are likely to be associated with the electrochemical double layer and with the polymer itself. For the blank measurement of the sample shown in Fig. 3a and b with a 1.0 mm radius, the fitted values are $R_1=0.419$ kΩ cm^2, $R_2=11.0$ kΩ cm^2, $C_1=86.9$ μF cm^{-2}, $Q_{CPE}=4.00$ μF s^{n-1}cm^{-2} and $n=0.774$, which corresponds to an estimated capacitance value of $C_2=0.620$ μF cm^{-2} by using the conversion $C_2=(R_2Q_{CPE})^{1/n}/R_2$ (Hsu and Mansfeld, 2001).

The high values of charge transfer resistance observed for the system, are compatible with the presence of the insulating polymer and the electrical potential barrier created by the negative charge of the aptamers towards the negatively charged redox markers in solution. As PSA binds to the cavities of the apta–MIP, less DNA charge is exposed to the outer electrolyte, causing a reduction in the resistance of the system. The screening of the charge of the PSA-specific DNA aptamer has previously been reported in the literature (Jolly et al., 2015b).

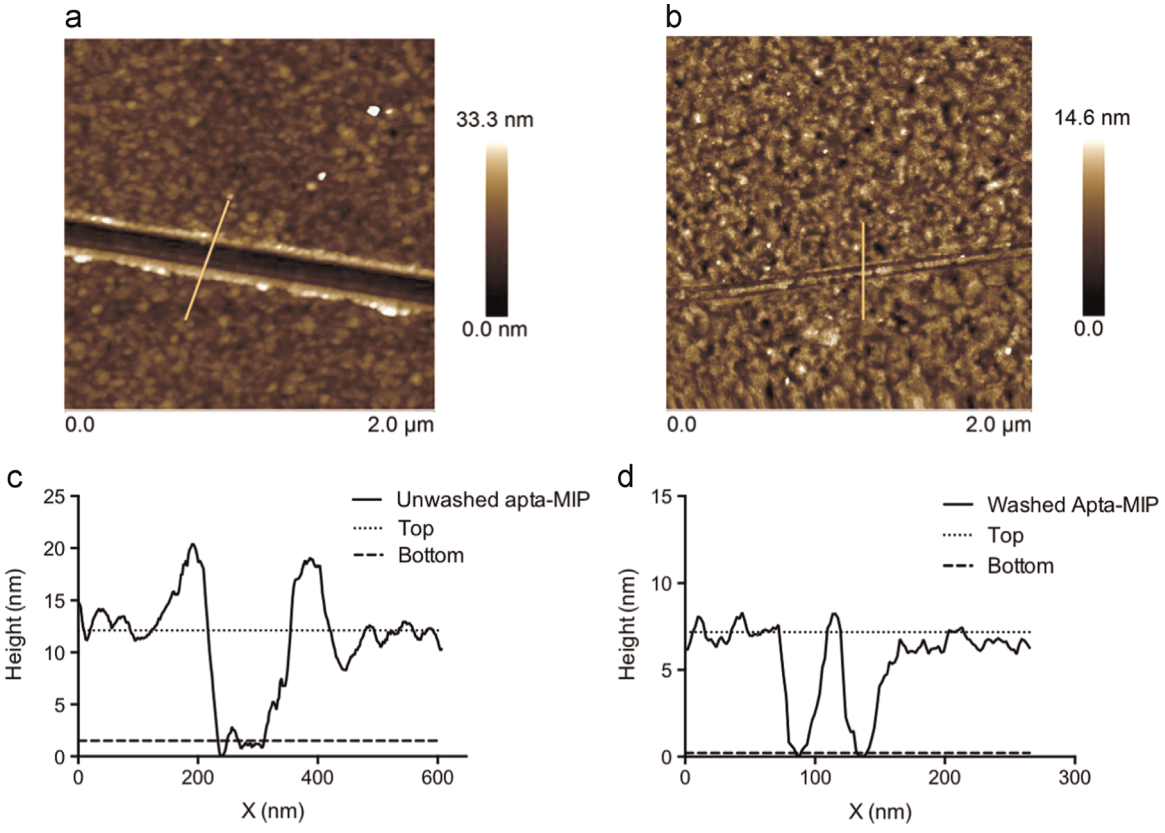

Fig. 2. AFM images (tapping mode) showing a planar gold surface following the formation of the apta–MIP layer before (a) and after (b) washing. Analysis of profiles across scratches in the polymer film suggest a thickness of 10.61 ± 1.23 nm before washing (c), which decreases to 7.49 ± 0.42 nm following washing (d).

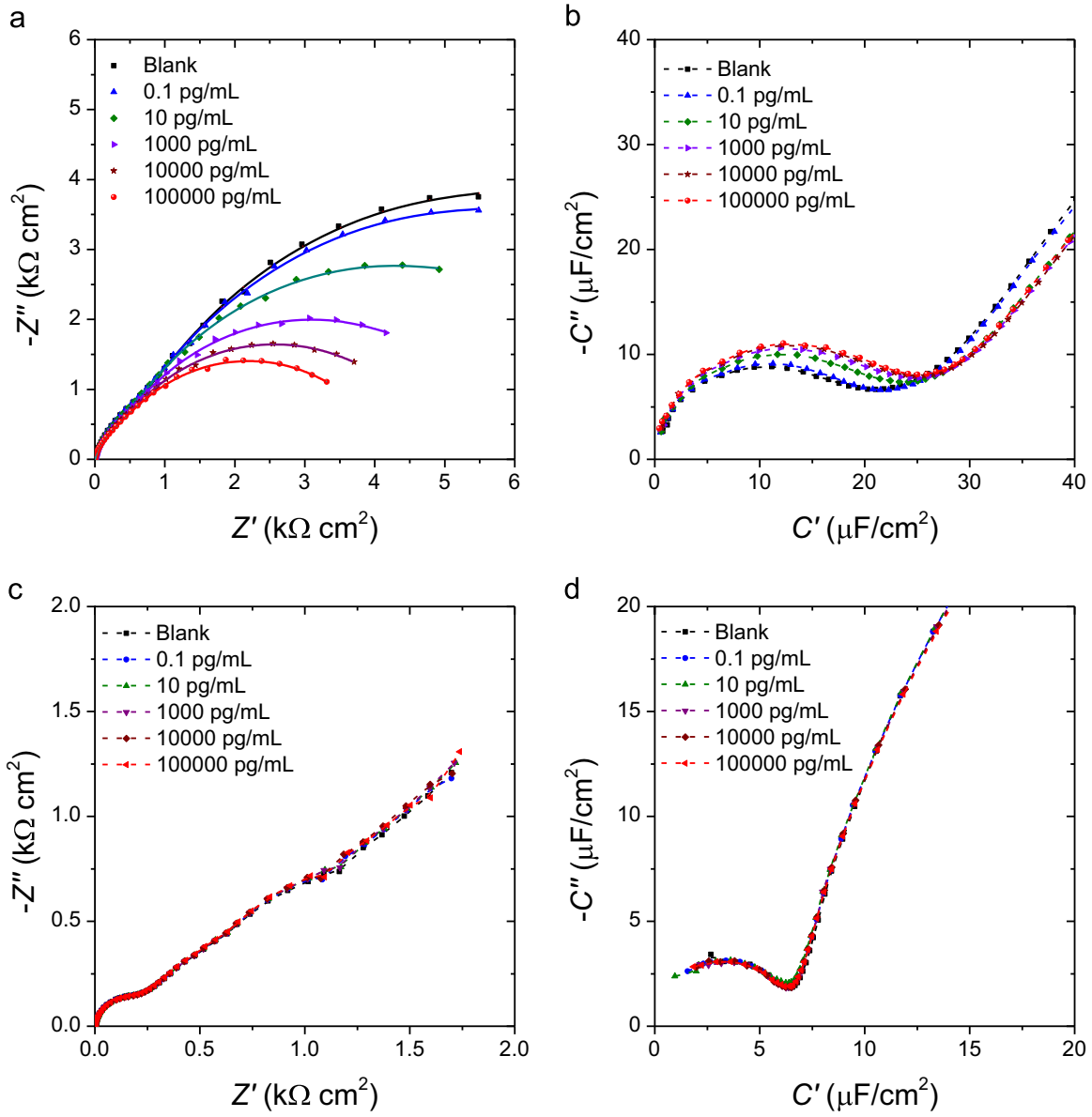

Fig. 3. Impedance Nyquist (a) and capacitance Cole–Cole (b) plots of the apta–MIP sensor incubated with different concentration of PSA. The lines in the Nyquist plot represent the fittings of the data with the equivalent circuit described. Impedance Nyquist (c) and capacitance Cole-Cole (b) plots of apta–NIP sensor incubated with different concentration of PSA.

Given the high impedance values of the system, a better evaluation of the capacitance of the system can be obtained by defining a complex capacitance

$$C^* = C' + jC'' \equiv \frac{1}{j\omega Z} = -\frac{Z''}{\omega |Z|^2} - j\frac{Z'}{\omega |Z|^2} \quad (1)$$

Fig. 3b shows the Cole–Cole capacitance plots at higher frequencies before and after PSA binding events; measurable changes in the capacitance are observed upon PSA interaction. The screening of the aptamer charges coupled with the filling of the polymer cavities could further explain the increase in capacitance of the system as PSA binds to the apta–MIP sensor. These changes were negligible in the apta–NIP sensor as shown in Fig. 3c and d demonstrating little PSA interaction with the control sensor surface (for full frequency range plots, before and after PSA binding to MIP and NIP, see Supporting information Section S4 and Figs. S5 and S6).

Due to the high impedance values of the system and the relatively low exponent n of the CPE, estimation of the capacitance of the system through fitting of the data with an equivalent circuit yields large errors. The errors are then exacerbated by the calculation of the capacitance through the fitted values of the constant phase element. Therefore we have used as our signal the measured impedance at a fixed frequency (1 Hz) so that the evolution of the signal can be monitored without the need for fitting. The capacitance, calculated as $C = -1/j\omega Z''$ at 1 Hz, for dose response with the apta–MIP and the apta–NIP sensor is shown in Fig. 4. Capacitance variations were obtained with respect to the baseline signal after achieving stability. The apta–MIP sensor incubated with 0.1 pg/ml PSA showed a capacitance change of 5% while 1 μg/ml PSA gave rise to a signal change of ~47% demonstrating high sensitivity in terms of sensor response. To put this result in to perspective, a closely analogous 'aptamer only' PSA sensor, also developed by our group using the same DNA aptamer (Jolly et al., 2015b), was shown to have a limit of detection of 1 ng/mL with a signal change ~3%. This suggests that the imprinting step resulted in an impressive increase in sensivity of around three orders of magnitude. The apta–MIP sensor showed a linear response from

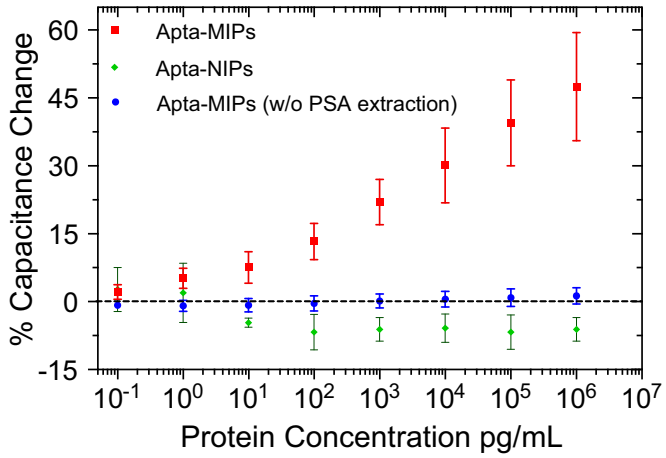

Fig. 4. Dose response of the apta–MIPs (red), apta–NIPs (green) and the apta–MIPs washed with water only (blue) with different concentrations of PSA. The horizontal dotted line represents the baseline signal. The capacitance values were calculated as $C=-1/j\omega Z''$ at 1 Hz. (For interpretation of the references to colour in this figure legend, the reader is referred to the web version of this article.)

100 pg/ml to 100 ng/ml PSA (Fig. 4, red data points), which encompasses the clinical range of PSA concentration used for PCa detection (4–10 ng/ml) (Heidenreich et al., 2014a). Control polymers, so-called apta–NIPs, were prepared in the same way but in the absence of PSA. The apta–NIPs showed a decrease in capacitance of up to 6% when incubated with 1 μg/ml PSA (Fig. 4, green data points). This is likely due to a small amount of non-specific interaction between PSA and the polydopamine film leading to an increase in the resistance to the flow of redox ions to the sensor surface. This large difference in the behaviour of the apta–NIP as compared to the apta–MIP is interesting; it strongly suggests that the binding of PSA to the aptamer *prior* to polymerisation somehow 'protects' the aptamer PSA binding site from 'denaturation' during polymer growth. To further explore our hybrid-MIP hypothesis an experiment was performed to evaluate the effect of the wash-step on the functioning of the apta–MIP. In the absence of acetic acid and SDS in the wash solution, it was proposed that template PSA would remain bound to the apta–MIP and would effectively prevent binding of additional PSA and this is exactly what was observed. Fig. 4 clearly shows (blue dots) that in the absence of acetic acid and SDS in the wash-step (template removal) the apta–MIP surface did not respond to PSA upon re-incubation. This strongly supports our hypothesis that reversible PSA binding or 'templating' protects the aptamer during polymerisation. This control study also eliminates the possibility that binding of PSA to the apta–MIP surface is a result of 'protein–protein' (PSA–PSA) binding. It is likely that the very weak response of the apta–NIP surface to PSA is due to the aptamer being 'overgrown' during polymerisation. It is probable that in the absence of a PSA template aptamer molecules pack more closely, and favour conformations that lie more closely to the gold surface when surface immobilised and as such become more vulnerable to polymer entrapment.

3.4. Evaluation of the selectivity of the apta–MIP

In order to evaluate the ability of the apta–MIP sensor to discriminate between PSA and other related proteins, the system was non-competitively challenged with human Kallikrein 2 protein (hK2). hK2 is a member of the same kallikrein family as PSA and is 80% homologous (Hong, 2014). Most antibodies raised against PSA exhibit cross-reactivity with hk2 due to similar epitopic regions and although the concentration of hK2 is 100 fold lower than PSA in clinical samples, this protein served as stringent control to evaluate apta–MIP selectivity (Väisänen et al., 2006). Upon incubation with increasing concentrations of hK2, the apta–MIP sensor exhibited a much reduced response as compared to PSA; approximately 10% (hK2) compared to 42% (PSA) signal change when incubated with 100 ng/ml of the respective proteins (Fig. 5a). (For the response of the apta–MIP sensor over the entire range of hK2 concentrations see Fig. S7 in Supporting information). The 'aptamer only' sensor gave a signal change of 1.6% with hK2 at 100 ng/ml while a signal change of 32% was observed with PSA (Jolly et al., 2015b). This suggests that PSA/hK2 aptamer selectivity has been to a degree lost in the imprinting step. An explanation for this might be that the aptamer relies on a small number of very specific and differentiating interactions between loci on the DNA and protein in order to discriminate between PSA and hK2. When the polymer layer builds it initially 'captures' the lower part of the aptamer–PSA complex. Given the assumption that the protein–aptamer complex is orientated so that the aptamer is closer to the electrode surface than the protein, the growing polymer layer builds around aptamer first, then the area of interaction between aptamer and protein and finally around the protein so that the polymer surrounds the parts of the protein that are furthest from the electrode surface. Given the homology between the two proteins and the generality of the non-covalent interactions established between polymer and protein it is not surprising that a large number of non-covalent interactions would not only result in increased affinity but also lead to reduced selectivity. The selectivity of the apta–MIP sensor could possibly be further improved by using electroactive monomers that display a higher

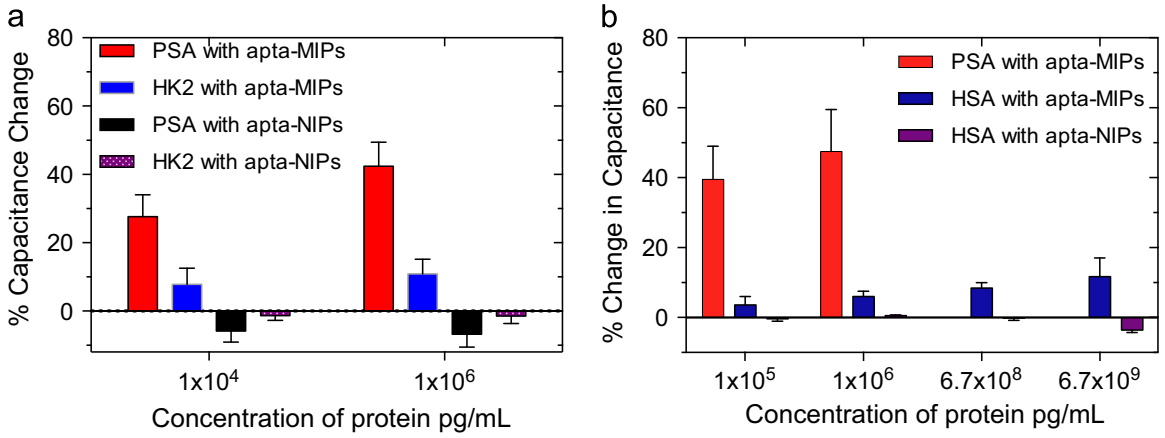

Fig. 5. Selectivity study of the apta–MIP with different concentrations of hK2 (a, blue) and HSA (b, blue) and respective PSA concentrations (red). (For interpretation of the references to colour in this figure legend, the reader is referred to the web version of this article.)

degree of functionality, hence allowing the receptors to be "tailored" to PSA. It might also be possible to carefully control the thickness of the polymer layer to achieve a balance between polymer–protein and aptamer–protein interactions. When the apta–NIPs were challenged with hK2 (100 ng/ml), a signal change of ~1.5% was observed which was lower than the PSA response of ~5%. The net charge of hK2 is negative, whereas at neutral pH the net charge of PSA is positive and this difference in charge is likely responsible for the difference in non-specific binding observed (Villoutreix et al., 1994). In the clinical setting, given the large difference in concentrations of the two proteins in the blood, significant interference from hK2 is unlikely (Väisänen et al., 2006).

Although the usefulness of PSA as a means to diagnose prostate cancer is questionable, it is important that any sensor developed for use within a clinical setting retains sensitivity when challenged with biological samples. The sensor was challenged with various concentrations of human serum albumin (HSA), the main plasma protein, in order to investigate potential fouling issues. HSA at 0.1 μg/ml and 1 μg/ml showed signal changes of 3% and 5% respectively (Fig. 5b). HSA is a negatively charged protein at pH 7.4 (Fogh-Andersen et al., 1993), which could lead to electrostatic repulsion between the polymer DNA layer and the protein resulting in low signal change. A maximum capacitive change of 11% was observed when the sensor was challenged with HSA at a concentration of 6.7 mg/ml (physiological range 3.5–5 mg/mL), which may result from a combination of non-specific interaction with polydopamine as well as protein–protein interactions. HSA interaction with apta–NIPs was similar to PSA interaction with apta–NIPs, showing negligible change at lower concentrations and an increase in capacitance with a signal change of 3.5% at 6.7 mg/ml HSA. These studies are encouraging, however, validation with clinical samples would be required to demonstrate true clinical utility.

This brings the discussion to the key point: 'is this evidence of a molecular imprinting effect?'. The mechanism underpinning the proposed hybrid MIP approach requires that the aptamer is restrained in a 'binding' conformation to deliver improvements in binding efficiency by thermodynamically favouring PSA binding to a conformationally restrained aptamer. It is hypothesised that improved affinity, and potentially selectivity, is a consequence of the aptamer and the polymer (MIP) acting synergistically. It is proposed that the polymer growth around the aptamer–PSA complex results in the aptamer being held in, or close to, its binding conformation following PSA removal. This restriction in free-movement of the aptamer reduces the entropy of the 'unbound' receptor favours rebinding by reducing the loss in entropy that would occur when PSA binds. There is also an argument for a reduction in enthalpy since there would be fewer non-covalent interactions between aptamer and polymer than would exist for the fully solvated form of the aptamer. In addition, it is reasonable that any reduction in aptamer solvation would also contribute to a reduction in PSA binding entropy loss. For this to happen template removal and subsequent re-binding must not be hampered by polymer-induced conformational restriction of the aptamer; there being an underlying assumption that binding-induced conformation changes, and the permanent capture of this conformation within a polymer support, does not result in permanent entrapment of the 'PSA' template. Fig. 4 suggests this is not the case since the ability to turn the affinity of the apta–MIP 'on' and 'off' by varying wash conditions is best explained in terms of the wash's ability to bring about template removal. This entrapment process itself could reasonably be described as 'imprinting' since the aptamer–PSA complex is effectively 'imprinted' within the polydopamine layer; even in the absence of any association between the PSA 'template' and the polymer. The proposed hybrid-MIP mechanism also requires that the polymer contributes to binding, in a typical non-covalent imprinting manner, by directly interacting with the template. Whether this happens to any great extent depends on the relative sizes of the aptamer and template and importantly on the thickness of the polymer layer. For instance if the template is a low molecular weight molecule, little interaction with the polymer might be expected as the aptamer when bound, effectively forms a shield around the molecule. If on the other hand the template is a similar or larger than the aptamer, then significant polymer interaction might be envisaged giving rise to an enhanced 'conventional' non-covalent imprinting effect. The polymer thickness also plays a critical role in the formation of the hybrid imprinted site and in this case, given the polymer thickness is roughly the size of the aptamer PSA template (9–10 nm) and that the 3D structure of PSA is larger than that of the aptamer, it is not unreasonable to assume that there would be significant direct interaction between the polymer and PSA.

So does the data demonstrate an imprinting effect? The data in Fig. 4 clearly shows that the apta–MIP has excellent sensitivity for PSA with a detection limit between 1 and 10 pg/ml, yet whilst this illustrates efficacy it is not direct evidence for an imprinting effect. The clearest evidence for a significant imprinting effect comes from the comparison with then previously published study (Jolly et al., 2015b) with the key observation being the large difference it the PSA limit of detection for the two systems. Whilst differences in aptamer surface-density and orientation would undoubtedly play some role in accounting for differences in performance it is very unlikely that at concentrations, for both systems, well below any observable saturation this could account for the difference observed. We therefore conclude that this improvement in the limit of detection for apta–MIP is the result of an imprinting contribution to the affinity of the system. Although it is clear that an imprinting effect has significantly improved the performance of the apta–MIP sensor compared to the aptasensor, it remains unclear as to whether this is the result of the conformational restriction of the aptamer, the establishment of non-covalent interactions between polymer and PSA or some combination of both.

4. Conclusions

By combining conventional bio-recognition motifs with molecular imprinting, a highly sensitive hybrid sensor has been generated. Using controlled electropolymerisation to bring about capture of the aptamer–PSA complex a three fold increase in sensitivity over a conventional aptasensor has been demonstrated, which is hypothesised to be a consequence of synergistic recognition of PSA by both the aptamer and the imprinted cavity. The sensor displayed good selectivity when challenged with a homologous protein hK2 and additionally good resistance to fouling from serum protein HSA. This strategy could be extended to various diagnostically relevant proteins using not only aptamers but also other affinity molecules such as peptides, affirmers and antibody fragments.

Acknowledgements

This work was funded by the European Commission Seventh Framework Programme through the Marie Curie Initial Training Network PROSENSE (Grant no. 317420, 2012–2016)

Appendix A. Supplementary information

Supplementary data associated with this article can be found in the online version at http://dx.doi.org/10.1016/j.bios.2015.08.043.

References

Bai, W., Spivak, D.A., 2014. A double-imprinted diffraction-grating sensor based on a virus-responsive super-aptamer hydrogel derived from an impure extract. Angew. Chem. 126, 2127–2130. http://dx.doi.org/10.1002/ange.201309462.

Ball, V., Frari, D.D., Michel, M., Buehler, M.J., Toniazzo, V., Singh, M.K., Gracio, J., Ruch, D., 2012. Deposition mechanism and properties of thin polydopamine films for high added value applications in surface science at the nanoscale. BioNanoScience 2, 16–34. http://dx.doi.org/10.1007/s12668-011-0032-3.

Bernsmann, F., Ponche, A., Ringwald, C., Hemmerlé, J., Raya, J., Bechinger, B., Voegel, J.-C., Schaaf, P., Ball, V., 2009. Characterization of dopamine – melanin growth on silicon oxide. J. Phys. Chem. C 113, 8234–8242. http://dx.doi.org/10.1021/jp901188h.

Blanco-López, M.C., Lobo-Castañón, M.J., Miranda-Ordieres, A.J., Tuñón-Blanco, P., 2004. Electrochemical sensors based on molecularly imprinted polymers. Trends Anal. Chem. 23, 36–48. http://dx.doi.org/10.1016/S0165-9936(04)00102-5.

Bowen, J.L., 2011. Detection of lipopolysaccharide pyrogens by molecularly imprinted polymers (PhD Thesis). Cardiff University, United Kingdom.

Dechtrirat, D., Gajovic-Eichelmann, N., Bier, F.F., Scheller, F.W., 2014. Hybrid material for protein sensing based on electrosynthesized MIP on a mannose terminated self-assembled monolayer. Adv. Funct. Mater. 24, 2233–2239. http://dx.doi.org/10.1002/adfm.201303148.

Fogh-Andersen, N., Bjerrum, P.J., Siggaard-Andersen, O., 1993. Ionic binding, net charge, and Donnan effect of human serum albumin as a function of pH. Clin. Chem. 39, 48–52.

Formisano, N., Jolly, P., Bhalla, N., Cromhout, M., Flanagan, S.P., Fogel, R., Limson, J.L., Estrela, P., 2015. Optimisation of an electrochemical impedance spectroscopy aptasensor by exploiting quartz crystal microbalance with dissipation signals. Sens. Actuators B 220, 369–375. http://dx.doi.org/10.1016/j.snb.2015.05.049.

Hayes, J.H., Barry, M.J., 2014. Screening for prostate cancer with the prostate-specific antigen test: a review of current evidence. J. Am. Med. Assoc. 311, 1143–1149. http://dx.doi.org/10.1001/jama.2014.2085.

Heidenreich, A., Bastian, P.J., Bellmunt, J., Bolla, M., Joniau, S., van der Kwast, T., Mason, M., Matveev, V., Wiegel, T., Zattoni, F., Mottet, N., 2014a. EAU guidelines on prostate cancer. Part 1: screening, diagnosis, and local treatment with curative intent—update 2013. Eur. Urol. 65, 124–137. http://dx.doi.org/10.1016/j.eururo.2013.09.046.

Heidenreich, A., Bastian, P.J., Bellmunt, J., Bolla, M., Joniau, S., van der Kwast, T., Mason, M., Matveev, V., Wiegel, T., Zattoni, F., Mottet, N., 2014b. EAU guidelines on prostate cancer. Part II: treatment of advanced, relapsing, and castration-resistant prostate cancer. Eur. Urol. 65, 467–479. http://dx.doi.org/10.1016/j.eururo.2013.11.002.

Ho, C.-C., Ding, S.-J., 2013. The pH-controlled nanoparticles size of polydopamine for anti-cancer drug delivery. J. Mater. Sci. – Mater. Med. 24, 2381–2390. http://dx.doi.org/10.1007/s10856-013-4994-2.

Hong, S.K., 2014. Kallikreins as biomarkers for prostate cancer. BioMed Res. Int. 2014, 526341. http://dx.doi.org/10.1155/2014/526341.

Hsu, C.H., Mansfeld, F., 2001. Concerning the conversion of the constant phase element parameter Y0 into a capacitance. Corrosion 57, 747–748.

Jolly, P., Formisano, N., Estrela, P., 2015a. DNA aptamer-based detection of prostate cancer. Chem. Pap. 69, 77–89. http://dx.doi.org/10.1515/chempap-2015-0025.

Jolly, P., Formisano, N., Tkáč, J., Kasák, P., Frost, C.G., Estrela, P., 2015b. Label-free impedimetric aptasensor with antifouling surface chemistry: a prostate specific antigen case study. Sens. Actuators B 209, 306–312. http://dx.doi.org/10.1016/j.snb.2014.11.083.

Keum, J.-W., Bermudez, H., 2009. Enhanced resistance of DNA nanostructures to enzymatic digestion. Chem. Commun. 45, 7036–7038. http://dx.doi.org/10.1039/B917661F.

Liu, K., Wei, W.-Z., Zeng, J.-X., Liu, X.-Y., Gao, Y.-P., 2006. Electrosynthesized polydopamine-imprinted film to the capacitive sensing of nicotine. Anal. Bioanal. Chem. 385, 724–729. http://dx.doi.org/10.1007/s00216-006-0489-z.

Liu, Y., Qiu, W.-Z., Yang, H.-C., Qian, Y.-C., Huang, X.-J., Xu, Z.-K., 2015. Polydopamine-assisted deposition of heparin for selective adsorption of low-density lipoprotein. RSC Adv. 5, 12922–12930. http://dx.doi.org/10.1039/C4RA16700G.

Łuczak, T., 2008. Preparation and characterization of the dopamine film electrochemically deposited on a gold template and its applications for dopamine sensing in aqueous solution. Electrochim. Acta 53, 5725–5731. http://dx.doi.org/10.1016/j.electacta.2008.03.052.

Lynge, M.E., Westen, R. van der, Postma, A., Städler, B., 2011. Polydopamine—a nature-inspired polymer coating for biomedical science. Nanoscale 3, 4916–4928. http://dx.doi.org/10.1039/C1NR10969C.

Maehashi, K., Katsura, T., Kerman, K., Takamura, Y., Matsumoto, K., Tamiya, E., 2007. Label-free protein biosensor based on aptamer-modified carbon nanotube field-effect transistors. Anal. Chem. 79, 782–787. http://dx.doi.org/10.1021/ac060830g.

McCauley, T.G., Hamaguchi, N., Stanton, M., 2003. Aptamer-based biosensor arrays for detection and quantification of biological macromolecules. Anal. Biochem. 319, 244–250.

Panasyuk, T.L., Mirsky, V.M., Piletsky, S.A., Wolfbeis, O.S., 1999. Electropolymerised molecularly imprinted polymers as receptor layers in capacitive chemical sensors. Anal. Chem. 71, 4609–4613. http://dx.doi.org/10.1021/ac9903196.

Poma, A., Brahmbhatt, H., Pendergraff, H.M., Watts, J.K., Turner, N.W., 2015. Generation of novel hybrid aptamer–molecularly imprinted polymeric nanoparticles. Adv. Mater. 27, 750–758. http://dx.doi.org/10.1002/adma.201404235.

Rodriguez, M.C., Kawde, A.-N., Wang, J., 2005. Aptamer biosensor for label-free impedance spectroscopy detection of proteins based on recognition-induced switching of the surface charge. Chem. Commun. 34, 4267–4269. http://dx.doi.org/10.1039/b506571b.

Savory, N., Abe, K., Sode, K., Ikebukuro, K., 2010. Selection of DNA aptamer against prostate specific antigen using a genetic algorithm and application to sensing. Biosens. Bioelectron. 26, 1386–1391. http://dx.doi.org/10.1016/j.bios.2010.07.057.

Turner, N.W., Jeans, C.W., Brain, K.R., Allender, C.J., Hlady, V., Britt, D.W., 2006. From 3D to 2D: a review of the molecular imprinting of proteins. Biotechnol. Prog. 22, 1474–1489. http://dx.doi.org/10.1021/bp060122g.

Väisänen, V., Peltola, M.T., Lilja, H., Nurmi, M., Pettersson, K., 2006. Intact free prostate-specific antigen and free and total human glandular kallikrein 2. Elimination of assay interference by enzymatic digestion of antibodies to F(ab′)2 fragments. Anal. Chem. 78, 7809–7815. http://dx.doi.org/10.1021/ac061201+.

Villoutreix, B.O., Griffin, J.H., Getzoff, E.D., 1994. A structural model for the prostate disease marker, human prostate-specific antigen. Protein Sci. 3, 2033–2044. http://dx.doi.org/10.1002/pro.5560031116.